

Optical Engineering

SPIDigitalLibrary.org/oe

Theoretical statistical relationships between the intensities of an image of the sea surface and its slopes: a result comparison of rect and Gaussian glitter functions

José Luis Poom-Medina
Josué Álvarez-Borrego
Beatriz Martín-Atienza
Ángel Coronel-Beltrán

Theoretical statistical relationships between the intensities of an image of the sea surface and its slopes: a result comparison of rect and Gaussian glitter functions

José Luis Poom-Medina,^a Josué Álvarez-Borrego,^{b,*} Beatriz Martín-Atienza,^c and Ángel Coronel-Beltrán^a

^aUniversity of Sonora, Physics Research Department, Rosales y Boulevard Luis Encinas S/N, Hermosillo, C. P. 83000, Mexico

^bCICESE, Applied Physics Division, Optics Department, Carretera Ensenada-Tijuana No. 3918, Fraccionamiento Zona Playitas, Ensenada, C. P. 22860, México

^cUABC, Faculty Marine Sciences, Carretera Ensenada-Tijuana Km. 103, Ensenada, C. P. 22860, México

Abstract. The reflection of the sunlight over the sea surface is called glitter pattern. In previous works where the one-dimensional case was analyzed, the glitter function was mathematically described by a rect function. This rect function has proven to be a very good representation of the glitter pattern. A Gaussian glitter function is used like a first approximation to the rect function. The statistical relationship between the variance and the correlation function of the intensities of the image, the glitter pattern, and the variance of the sea surface slopes are obtained and analyzed. The analytical solutions for these relationships are given by different equations; however, the graphic representations are very similar. © The Authors. Published by SPIE under a Creative Commons Attribution 3.0 Unported License. Distribution or reproduction of this work in whole or in part requires full attribution of the original publication, including its DOI. [DOI: 10.1117/1.OE.53.4.043103]

Keywords: sea surface; inverse problem; image processing; glitter pattern.

Paper 131810P received Nov. 29, 2013; revised manuscript received Feb. 21, 2014; accepted for publication Mar. 5, 2014; published online Apr. 2, 2014.

1 Introduction

To measure the wave motion, the use of radar images and optical processing of aerial photographs has been used. In the last century, Barber¹ showed that the periodicity and directionality of waves can be estimated from the optical diffraction patterns of an image of the sea surface. Cox and Munk²⁻⁴ studied the distribution of intensity or glitter patterns in aerial photographs of the sea. One of their conclusions was that for constant and moderate wind speed, the probability density function of the slopes is Gaussian as a first approximation. This could be taken as an indication that in certain circumstances the ocean surface could be modeled as a Gaussian random process.

Álvarez-Borrego⁵⁻⁷ derived the equations which describe the glitter pattern in one and two dimensions. With the glitter function, we can find the variance and the correlation function of the sea surface slopes from the statistics of the intensities in the image. Álvarez-Borrego⁸ considered the problem of retrieving spatial information of the statistical properties of random rough sea surfaces from images via remote sensing. He obtained expressions relating the variance and the correlation function in the image and the surface heights. He considered the detector located at an arbitrary height above the sea level.

Zhang and Wang⁹ carried out comparison studies with measurements from moderate resolution imaging spectroradiometer for several popular sun glitter models.

Baxter¹⁰ studied the ocean wave slope and height retrieval using imagery collected from a polarimetric camera system mounted on an airborne platforms, enabling measurements

over large areas and in regions devoid of wave buoys developing a technique to calculate significant wave height.

Kay et al.¹¹ demonstrated that it is feasible to generate high-resolution sea surface models and use them in radiative transfer modeling of the ocean surface. Incorporating correct statistics of surface elevation as well as slope gave estimates of reflected radiance.

Recently, an improved model to obtain some statistical properties of the sea surface slopes via remote sensing using variable reflection angle has been considered.¹² The statistical parameters of the sea surface slopes were obtained from the statistics of the glitter pattern considering the detector located at any heights over the mean of the sea level.

In the present article, we derive new relationships of the variance and the correlation function of the intensities in the image of the sea surface and sea surface slopes for different incidence angles by considering a Gaussian glitter function. We also compare these results with the obtained previously by Álvarez-Borrego and Martín-Atienza.¹² In other words, illumination changes in the glitter pattern can be modeled using a Gaussian glitter function and the comparison with previous result will give us an idea about the behavior of these theoretical relationships. In our work, we assume that all the sea waves are moving along a single direction (in the open ocean the wind waves can be assumed to be mono-directional, however, this is not true for shallow environments because of the varied topography¹³) and vertical plane containing this direction includes both the observer and the sun.¹⁴ However, for any angle of reflection of the sunlight, the glint points on one transect taken from a two-dimensional glitter image does not contain the same number of glitter as a one-dimensional (1-D) profile because of the x and y components.

*Address all correspondence to: Josué Álvarez-Borrego, E-mail: josue@cicese.mx

The material of this work is organized as follows: in Sec. 2, the statistical properties of sea surface slopes are described; in Sec. 2.1, the statistical properties using a rect glitter function are obtained; in Secs. 2.1.1 and 2.1.2, the relationships among the variances and the correlation function of the intensities in the image and sea surface slopes considering a Gaussian probability density function are calculated, respectively; in Sec. 2.2, the statistical properties using a Gaussian glitter function like the mean, variance, and the correlation function of the image are obtained; in Sec. 3, the results and discussions are presented and in Sec. 4, the conclusions are given.

2 Statistical Properties of Sea Surface Slopes

This section describes the geometric model used and the different theoretical relationships between the variances and the correlation functions using different glitter function.

2.1 1-D Geometric Model

We propose to use the same 1-D geometry as in Álvarez-Borrego and Martín-Atienza,¹² in which θ_d is a variable angle subtended by the optical system of the detector with the normal at one point of the surface (Fig. 1). This model does not impose a restriction on the sensor field of view. In addition, we neglect the effect of shadowing, i.e., when some reflecting points are obscured by roughness of the sea surface.

The geometric model, considering θ_d as a variable, is shown in Fig. 1. The surface $\zeta(x)$ is illuminated by a uniform incoherent source S of limited angular extent, with wavelength λ and an apparent diameter β . Its image is formed in D by an aberration free optical system. The incidence angle θ_s is defined as the angle between the incidence direction and the normal to the mean surface. From Fig. 1, we can observe that, $(\theta_d)_i$ corresponds to the angle subtended by the optical system of the detector with the normal to the point i of the surface, and is given by

$$(\theta_d)_i = \tan^{-1}\left(\frac{i\Delta x}{H}\right), \tag{1}$$

where H are the height of the detector, and Δx is the interval between surface points. Here, α_i is the slope angle at each i point in the surface and is subtended between the normal to the mean surface and the normal to the surface in the i point, i.e.,

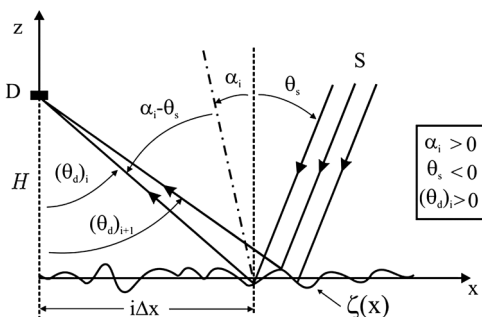


Fig. 1 Geometry of the model to get some statistical properties of marine surface.

$$\alpha_i = \frac{\theta_s}{2} + \frac{1}{2} \tan^{-1}\left(\frac{i\Delta x}{H}\right). \tag{2}$$

In this realistic physical situation, the angle $(\theta_d)_i$ is changing with respect to each point in the surface. It is worth noticing that by using a variable $(\theta_d)_i$ the sensor field of view is not restricted.

According to Álvarez-Borrego and Martín-Atienza,¹² the glitter function can be expressed as

$$B(M_i) = \text{rect}\left[\frac{M_i - M_{0i}}{(1 + M_{0i}^2)\frac{\beta}{2}}\right], \tag{3}$$

where

$$M_{0i} - (1 + M_{0i}^2)\frac{\beta}{4} \leq M_i \leq M_{0i} + (1 + M_{0i}^2)\frac{\beta}{4}, \tag{4}$$

$$M_i = \tan(\alpha_i), \tag{5}$$

$$M_{0i} = \tan\left[\frac{\theta_s + (\theta_d)_i}{2}\right]. \tag{6}$$

By combining Eqs. (2) and (4)–(6), we obtained

$$\frac{\theta_s}{2} + \frac{1}{2} \tan^{-1}\left(\frac{i\Delta x}{H}\right) - \frac{\beta}{4} \leq \alpha_i \leq \frac{\theta_s}{2} + \frac{1}{2} \tan^{-1}\left(\frac{i\Delta x}{H}\right) + \frac{\beta}{4}, \tag{7}$$

which is the slope angle interval, where a bright spot is received by the sensor.

2.1.1 Relationship between the variance of the intensities in the image and surface slopes considering the Gaussian probability density function for the slopes and using the rect glitter function

The mean of the image μ_I may be written as¹²

$$\begin{aligned} \mu_I &= \frac{1}{N} \sum_{i=1}^N \int_{-\infty}^{\infty} B(M_i) p(M_i) dM_i \\ &= \frac{1}{N} \sum_{i=1}^N \frac{1}{\sigma_M \sqrt{2\pi}} \int_{-\infty}^{\infty} \text{rect}\left[\frac{M_i - M_{0i}}{(1 + M_{0i}^2)\frac{\beta}{2}}\right] \exp\left(-\frac{M_i^2}{2\sigma_M^2}\right) dM_i, \end{aligned} \tag{8}$$

where $p(M_i)$ is the Gaussian probability density function in one dimension. Defining $L_{1i} = M_{0i} - (1 + M_{0i}^2)\beta/4$ and $L_{2i} = M_{0i} + (1 + M_{0i}^2)\beta/4$ the resulting expression is

$$\mu_I = \frac{1}{N} \sum_{i=1}^N \frac{1}{2} \left[\text{erf}\left(\frac{L_{2i}}{\sqrt{2}\sigma_M}\right) - \text{erf}\left(\frac{L_{1i}}{\sqrt{2}\sigma_M}\right) \right]. \tag{9}$$

The variance of the intensities in the image is defined by Álvarez-Borrego and Martín-Atienza:¹²

$$\begin{aligned} \sigma_I^2 &= \frac{1}{N} \sum_{i=1}^N \int_{-\infty}^{\infty} [B(M_i) - \mu_I]^2 p(M_i) dM_i \\ &= \frac{1}{N} \sum_{i=1}^N \left\{ \frac{1}{2} \left[\operatorname{erf} \left(\frac{L_{2i}}{\sqrt{2}\sigma_M} \right) - \operatorname{erf} \left(\frac{L_{1i}}{\sqrt{2}\sigma_M} \right) \right] \right. \\ &\quad \left. - \frac{1}{4N} \left[\operatorname{erf} \left(\frac{L_{2i}}{\sqrt{2}\sigma_M} \right) - \operatorname{erf} \left(\frac{L_{1i}}{\sqrt{2}\sigma_M} \right) \right]^2 \right\}, \end{aligned} \quad (10)$$

which is the required relation between the variance of the intensities in the image, σ_I^2 , and the variance of the surface slopes, σ_M^2 .

2.1.2 Relationship between the correlation function of the intensities in the image and surface slopes considering the Gaussian probability density function for the slopes and the rect glitter function

The relationship between the correlation function of the surface slopes, $C_M(\tau)$, and the correlation function of the glitter pattern, $C_I(\tau)$, is given by

$$\begin{aligned} \sigma_I^2 C_I(\tau) &= \frac{1}{N} \sum_{j=1}^N \int_{-\infty}^{\infty} \frac{1}{N} \sum_{i=1}^N \int_{-\infty}^{\infty} B(M_{1i}) B(M_{2j}) \\ &\quad \times p(M_{1i}, M_{2j}) dM_{1i} dM_{2j}, \end{aligned} \quad (11)$$

where τ is the lag and $B(M_{1i})$ and $B(M_{2j})$ are the glitter function in two different slopes, and

$$\begin{aligned} p(M_{1i}, M_{2j}) &= \frac{1}{2\pi\sigma_M^2 [1 - C_M^2(\tau)]^{1/2}} \\ &\quad \times \exp \left\{ -\frac{M_{1i}^2 + M_{2j}^2 - 2C_M(\tau)M_{1i}M_{2j}}{2\sigma_M^2 [1 - C_M^2(\tau)]} \right\} \end{aligned} \quad (12)$$

and after an analytical integration we obtain

$$\begin{aligned} \sigma_I^2 C_I(\tau) &= \frac{1}{N^2} \sum_{j=1}^N \int_{L_{1j}}^{L_{2j}} \sum_{i=1}^N \frac{\sqrt{2}}{4\sigma_M\sqrt{\pi}} \exp \left[-\frac{M_{2j}^2}{2\sigma_M^2} \right] \\ &\quad \times \left\{ \operatorname{erf} \left(\frac{L_{2i} - C_M(\tau)M_{2j}}{\sqrt{2}\sigma_M [1 - C_M^2(\tau)]} \right) \right. \\ &\quad \left. - \operatorname{erf} \left(\frac{L_{1i} - C_M(\tau)M_{2j}}{\sqrt{2}\sigma_M [1 - C_M^2(\tau)]} \right) \right\} dM_{2j}, \end{aligned} \quad (13)$$

and $L_{1j} = M_{0j} - (1 + M_{0j}^2)(\beta/4)$, $L_{2j} = M_{0j} + (1 + M_{0j}^2) \times (\beta/4)$ and $M_{0j} = \tan\{[\theta_s + (\theta_d)_j]/2\}$.

Equation (13) is the required relation between the correlation function of the intensities in the image, $C_I(\tau)$, and the correlation function of the surface slopes, $C_M(\tau)$.

2.2 Relationship between the Variance and the Correlation Functions of the Intensities in the Image with Sea Surface Slopes Considering the Gaussian Probability Density Function and Using the Gaussian Glitter Function

In this article, we define the Gaussian glitter function as

$$B(M_i) = \exp \left[-\frac{(M_i - M_{0i})^2}{a_i^2} \right], \quad (14)$$

and considering Eqs. (4)–(7), and the same definition for the mean and the variance of the intensities of the image, we find

Table 1 Variances of the image for different incidence angles, when $H = 100, 500, 1000,$ and 5000 m.

θ_s (deg)	Theoretical variance of the image	Mean theoretical variance
100 m		
10	0.001069765223863	0.001064441599496
20	0.001492025954505	0.001487184949989
30	0.001958230130476	0.001955343259637
40	0.002388736757325	0.002388029903017
50	0.002671209128861	0.002671295526859
500 m		
10	0.003108873399102	0.003110830998389
20	0.003208815843187	0.003211731390714
30	0.002889310589063	0.002891047686755
40	0.0002257519594897	0.002257332274056
50	0.001511883141621	0.001510770353073
1000 m		
10	0.003378318252945	0.003381503619410
20	0.003092065713698	0.003094688190786
30	0.002426914586206	0.002428151612356
40	0.001608171050977	0.001608346018891
50	8.760812803764654e – 004	8.759361191028363e – 004
5000 m		
10	0.003275186586775	0.003278138111697
20	0.002669361095169	0.002671306656354
30	0.001833467188234	0.001834361752515
40	0.001032391737440	0.001032663417692
50	4.561791395959260e – 004	4.562286393551489e – 004

$$\mu_I = \frac{1}{N} \sum_{i=1}^N \left(\frac{a_i}{2\sqrt{2\sigma_M^2+a_i^2}} \exp \left[-\frac{M_{0i}^2}{2\sigma_M^2+a_i^2} \right] \times \left\{ \begin{array}{l} \operatorname{erf} \left[\frac{\sqrt{2\sigma_M^2+a_i^2}}{\sqrt{2a_i\sigma_M}} (L_{2i}) - \frac{\sqrt{2}\sigma_M M_{0i}}{a_i\sqrt{2\sigma_M^2+a_i^2}} \right] - \\ \operatorname{erf} \left[\frac{\sqrt{2\sigma_M^2+a_i^2}}{\sqrt{2a_i\sigma_M}} (L_{1i}) - \frac{\sqrt{2}\sigma_M M_{0i}}{a_i\sqrt{2\sigma_M^2+a_i^2}} \right] \end{array} \right\} \right), \quad (15)$$

and

$$\sigma_I^2 = \frac{1}{N} \sum_{i=1}^N \frac{a_i}{2\sqrt{4\sigma_M^2+a_i^2}} \exp \left[-\frac{2M_{0i}^2}{4\sigma_M^2+a_i^2} \right] \times \left\{ \begin{array}{l} \operatorname{erf} \left[\left(\frac{\sqrt{4\sigma_M^2+a_i^2}}{\sqrt{2a_i\sigma_M}} \right) (L_{2i}) - \frac{2\sqrt{2}\sigma_M M_{0i}}{a_i\sqrt{4\sigma_M^2+a_i^2}} \right] - \\ \operatorname{erf} \left[\left(\frac{\sqrt{4\sigma_M^2+a_i^2}}{\sqrt{2a_i\sigma_M}} \right) (L_{1i}) - \frac{2\sqrt{2}\sigma_M M_{0i}}{a_i\sqrt{4\sigma_M^2+a_i^2}} \right] \end{array} \right\} - \mu_I^2, \quad (16)$$

where $a_i = (1 + M_{0i}^2)\beta/8$ gives information of the width of the Gaussian glitter function.

In addition, the relationship between the correlation function of the surface slopes, $C_M(\tau)$, and the correlation function of the glitter pattern, $C_I(\tau)$, is given by

$$\sigma_I^2 C_I(\tau) = \frac{1}{N^2} \sum_{j=1}^N \int_{L_{1j}}^{L_{2j}} \sum_{i=1}^N \frac{a_i}{2\sqrt{2\pi\sigma_M} \sqrt{a_i^2 + 2\sigma_M^2[1 - C_M^2(\tau)]}} \times \exp \left(\begin{array}{l} \left(\frac{-a_i^2 a_j^2 - 2\sigma_M^2 \{a_i^2 + a_j^2 + 2\sigma_M^2 [1 - C_M^2(\tau)]\}}{2a_i^2 \sigma_M^2 \{a_i^2 + 2\sigma_M^2 [1 - C_M^2(\tau)]\}} \right) M_{2j}^2 + \\ + \left\{ \frac{2M_{0i} C_M(\tau)}{a_i^2 + 2\sigma_M^2 [1 - C_M^2(\tau)]} + \frac{2M_{0j}}{a_j^2} \right\} M_{2j} + \frac{2M_{0i}^2}{a_i^2} \left\{ \frac{\sigma_M^2 [1 - C_M^2(\tau)]}{a_i^2 + 2\sigma_M^2 [1 - C_M^2(\tau)]} - \frac{1}{2} \right\} - \frac{M_{0j}^2}{a_j^2} \end{array} \right) \times \left(\begin{array}{l} \operatorname{erf} \left\{ \frac{a_i (M_{0i} - C_M(\tau) M_{2j})}{\sigma_M \sqrt{2[1 - C_M^2(\tau)]} \sqrt{a_i^2 + 2\sigma_M^2 [1 - C_M^2(\tau)]}} + \frac{\sqrt{a_i^2 + 2\sigma_M^2 [1 - C_M^2(\tau)]} (L_{2i} - M_{0i})}{a_i \sigma_M \sqrt{2[1 - C_M^2(\tau)]}} \right\} \\ - \operatorname{erf} \left\{ \frac{a_i (M_{0i} - C_M(\tau) M_{2j})}{\sigma_M \sqrt{2[1 - C_M^2(\tau)]} \sqrt{a_i^2 + 2\sigma_M^2 [1 - C_M^2(\tau)]}} + \frac{\sqrt{a_i^2 + 2\sigma_M^2 [1 - C_M^2(\tau)]} (L_{1i} - M_{0i})}{a_i \sigma_M \sqrt{2[1 - C_M^2(\tau)]}} \right\} \end{array} \right) dM_{2j}. \quad (20)$$

Although we obtain an analytical relationship for the first integral, for the second integral, the process must be numeric. In order to avoid computer memory problems, the 16,000 data-point profile can be divided into 16 consecutive intervals. The value of $(\theta_d)_i$ varies point to point in the profile. For each interval and for each θ_s value, the relationship between the correlation functions $C_I(\tau)$ and $C_M(\tau)$ is calculated. Then, to compare the results using the rect and the Gaussian glitter function we used a value of $\sigma_M = 0.2121$. It is necessary to normalize the correlation functions, by using the corresponding variances. A theoretical variance σ_I^2 can be calculated from Eqs. (10) and (16) (for both rect and Gaussian glitter function cases), respectively. It is also possible to estimate the variance by averaging the theoretical variances calculated for each of the 16 intervals. In the rect glitter function case, these results can be seen in Álvarez-Borrego and Martín-Atienza.¹² We compare both variances in Table 1 for the Gaussian glitter function case for different values of H .

$$\sigma_I^2 C_I(\tau) = \frac{1}{N} \sum_{j=1}^N \int_{-\infty}^{\infty} \frac{1}{N} \sum_{i=1}^N \int_{-\infty}^{\infty} \frac{B(M_{1i})B(M_{2j})}{2\pi\sigma_M^2 [1 - C_M^2(\tau)]^{1/2}} \times \exp \left\{ -\frac{M_{1i}^2 + M_{2j}^2 - 2C_M(\tau)M_{1i}M_{2j}}{2\sigma_M^2 [1 - C_M^2(\tau)]} \right\} dM_{1i} dM_{2j}, \quad (17)$$

where

$$B(M_{1i})B(M_{2j}) = \exp \left[-\frac{(M_{1i} - M_{0i})^2}{a_i^2} \right] \exp \left[-\frac{(M_{2j} - M_{0j})^2}{a_j^2} \right], \quad (18)$$

and

$$p(M_{1i}, M_{2j}) = \frac{1}{2\pi\sigma_M^2 [1 - C_M^2(\tau)]^{1/2}} \times \exp \left\{ -\frac{M_{1i}^2 + M_{2j}^2 - 2C_M(\tau)M_{1i}M_{2j}}{2\sigma_M^2 [1 - C_M^2(\tau)]} \right\} dM_{1i} dM_{2j}. \quad (19)$$

Therefore, the result of the first integral is

3 Results and Discussions

The next figures show the comparison of Eqs. (10) and (13), where the rect function and the Gaussian function are used like glitter functions.

In Fig. 2, the variance of the surface slope is represented against the variance of the intensities of the image. Values of σ_M^2 from 0 to 0.04 correspond linearly to a wind velocity in the range from 0 to 12 to 14 m/s, according to Cox and Munk.¹⁵ The shape of the curves for the rect and the Gaussian cases is very similar. Their differences correspond to the changes in the values of the variance of the intensities. The profile of the source in the Gaussian case is less intense than for the rect glitter function. This figure shows how these relationships change for different heights (100, 500, 1000, and 5000 m). It can be seen that when H increases, the line corresponding to a value of incidence angle of 50 deg descends and even cross with the others lines.

When H increases, the lines with larger θ_s go down until the arrangement of the curves changes. If the camera is fixed

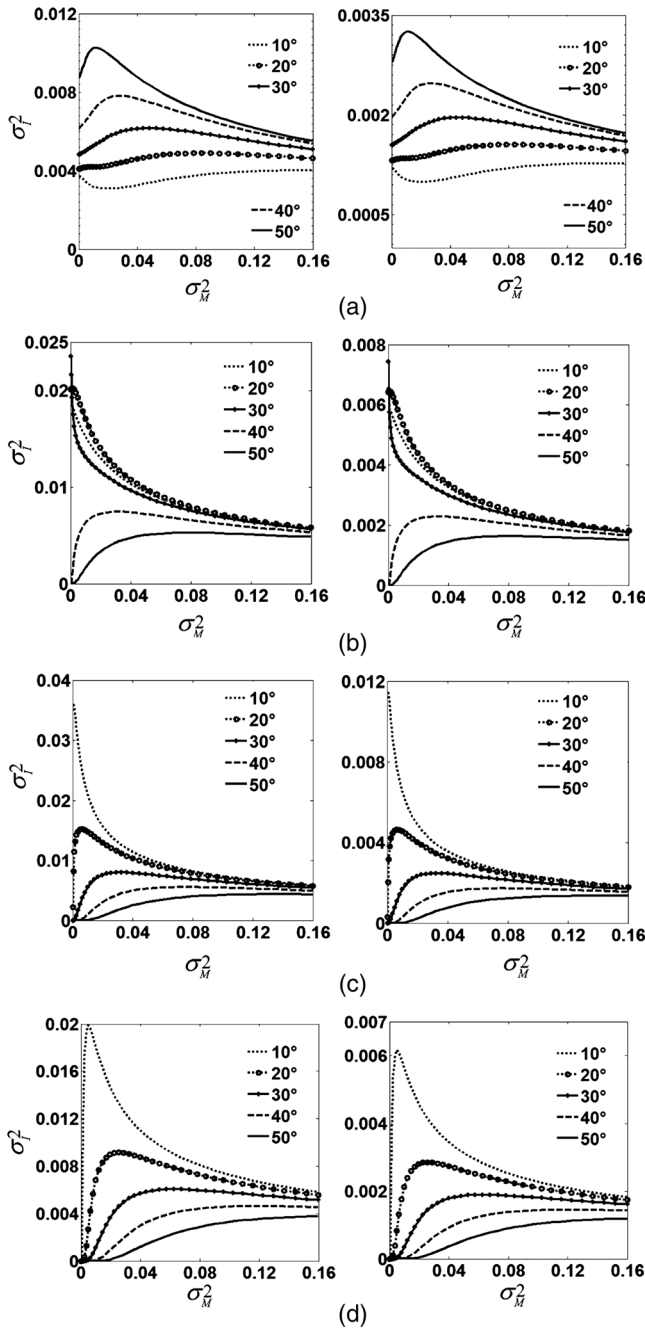


Fig. 2 Comparison between the variance of the intensities of the image versus the variance of the surface slopes using rect (left side) and Gaussian (right side) glitter function for: H : (a) 100, (b) 500, (c) 1000, and (d) 5000 m, respectively.

at $H = 100$ m, it will receive more reflected light at large θ_s because of the geometry of the reflection. When H increases, the camera sensor will receive less reflected light for large incidence angles.

In Fig. 3, the shape of the curves is also very similar for the rect and Gaussian cases (excepting for $H = 100$ m). This figure shows these normalized relationships using the two glitter functions) for 100, 500, 1000, and 5000 m. The correlation functions have a behavior similar to the variance curves when the sensor height changes.

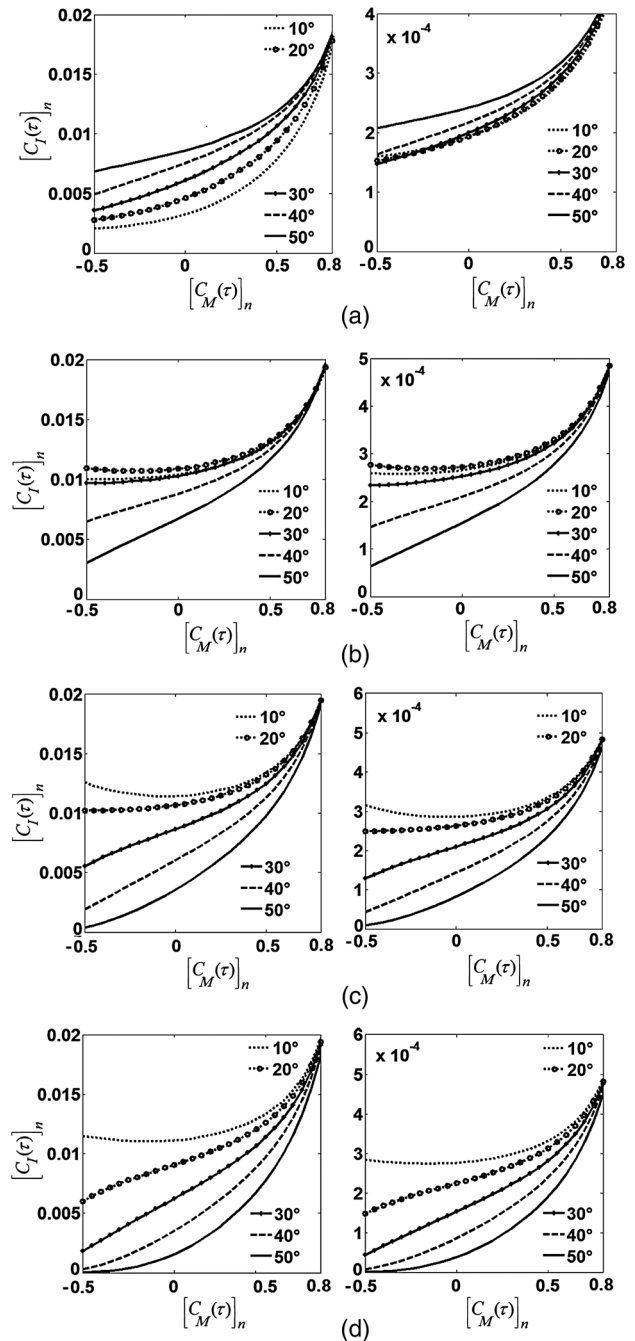


Fig. 3 Comparison between the correlation of the intensities of the image versus the correlation of the surface slopes, using rect (left side) and Gaussian (right side) glitter function for H : (a) 100, (b) 500, (c) 1000, and (d) 5000 m, respectively.

4 Conclusions

The behavior of the curves for different H is the same, notwithstanding the use of the rect or the Gaussian glitter function. Both glitter functions are easy to use in the calculations of these relationships. The differences in the values of the variance of the intensities of the image in both cases are proportional to the profile of the source used. Both glitter functions represent well the physics of the problem, which can act as a function to modulate the intensity of luminescence on brightness pattern, which is consistent with different

actual physical situation such as the presence of clouds or aerosols between the sensor and sensing area of sea surface.

Acknowledgments

This document is based on work partially supported by CONACYT under Grant 102007 and 169174 and mixed Scholarships 2013-mzo 2014 for national mobility in México.

References

1. N. F. Barber, "Finding the direction of travel of sea waves," *Nature* **174**, 1048–1050 (1954).
2. C. Cox and W. Munk, "Measurement of the roughness of the sea surface from photographs of the sun's glitter," *J. Opt. Soc. Am.* **44**(11), 838–850 (1954).
3. C. Cox and W. Munk, "Statistics of the sea surface derived from sun glitter," *J. Mar. Res.* **13**, 198–227 (1954).
4. C. Cox and W. Munk, "Some problems in optical oceanography," *J. Mar. Res.* **14**, 381–396 (1955).
5. J. Álvarez-Borrego, "Wave height spectrum from sun glint patterns: an inverse problem," *J. Geophys. Res.* **98**(C6), 10245–10258 (1993).
6. J. Álvarez-Borrego, "Two dimensional glitter function in the study of rough surfaces via remote sensing," *J. Mod. Opt.* **40**(11), 2081–2086 (1993).
7. J. Álvarez-Borrego, "1-D rough surfaces: glitter function for remote sensing," *Opt. Commun.* **113**(4–6), 353–356 (1995).
8. J. Álvarez-Borrego, "Some statistical properties of surface heights via remote sensing," *J. Mod. Opt.* **42**(2), 279–288 (1995).
9. H. Zhang and M. Wang, "Evaluation of sun glint models using MODIS measurements," *J. Quant. Spectrosc. Radiat. Transfer* **111**(3), 492–506 (2010).
10. R. Baxter, "Ocean wave slope and height retrieval using airborne polarimetric remote sensing," Ph.D. Thesis, Georgetown University (2012).
11. S. Kay et al., "Light transfer at the ocean surface modeled using high resolution sea surface realizations," *Opt. Express* **19**(7), 6493–6504 (2011).
12. J. Álvarez-Borrego and B. Martín-Atienza, "An improved model to obtain some statistical properties of surface slopes via remote sensing using variable reflection angle," *IEEE Trans. Geosci. Remote Sens.* **48**(10), 3647–3651 (2010).
13. E. J. Hochberg, "HyspIRI sun glint report," Technical Report, JPL Publication 11-4 (2011).

14. J. Álvarez-Borrego and B. Martín-Atienza, "Some statistical properties of surface slopes via remote sensing using variable reflection angle considering a non-Gaussian probability density function," *IEEE Geosci. Remote Sens. Lett.* **10**(2), 246–250 (2013).
15. C. Cox and W. Munk, "Slopes of the sea surface deduced from photography of sun glitter," *Bull. Scripps Inst. Oceanogr.* **6**(5), 397–487 (1956).

José Luis Poom-Medina is a PhD student at the University of Sonora México with a major in physics. He received his BS and MS degrees in physics and applied mathematics from the University of Sonora and University of Guadalajara in 1989 and 2004, respectively. He is a student member of SPIE.

Josué Álvarez-Borrego received his BS degree in physical oceanography in 1981 from the Facultad de Ciencias Marinas, Ensenada, Baja California, México, and his MSc and PhD degrees in optics in 1983 and 1993 from CICESE, Mexico. He is a professor with the Applied Physics Division, Optics Department, CICESE, México. His research interests are image processing with applications to biogenic particles and image processing of the sea surface. He is a member of the Mexican Academy of Optics, National Research System (SNI), and the Mexican Sciences Academy.

Beatriz Martín-Atienza received her BS (1993) in physics and a PhD (2001) in physics from Universidad Complutense de Madrid, Spain. She worked at the Earth Sciences Division, Applied Geophysics Department, CICESE, Baja California, Mexico, for 2 years (2001 to 2003) as an associate researcher. Since 2004, she has been working at the Facultad de Ciencias Marinas, UABC, Baja California, Mexico, teaching physics and mathematics courses in oceanology. Her research interests include inversion of oceanological and geophysical data and image processing of the sea surface.

Ángel Coronel-Beltrán is a titular researcher at the Departamento de Investigación en Física, Universidad de Sonora, México. He received his BS degree in physics in 1983 from the Universidad de Sonora, México, and his MSc degree in optics in 1988 from CICESE, México, and his PhD degree in sciences in 2010 from UABC, México. His current research interests are image processing and invariant correlation digital systems. He is a member of the Mexican Academy of Optics and the Mexican Physical Society.